The Electric Arc As a Circuit Component

Conference Paper · November 2015

DOI: 10.1109/IECON.2015.7392564

Jonathan Andrea
Esterline Technologies Corporation

The Electric Arc as a Circuit Component

Jonathan Andrea, Patrick Besdel, Olivier Zirn, Marc Bournat
Secondary Electrical Distribution Departement
Esterline Power Systems, Sarralbe, France

***Abstract*—This paper presents a mathematical model which describes the behavior of the electric arc in power circuits. The arc is studied like a circuit component. Arc equations are analyzed for static and dynamic situations to define a small signal model. Simulation results and experimental results are given for common arc ignition cases.**

***Keywords*—The Electric Arc, Arc Model, Arc Equation, Arc Fault, Component, Circuit.**

I. Introduction

The electric arc is commonly used for welding [1], for cutting [2], for furnaces [3], for lighting [4]. It is used to produce carbon nanotubes [5], for mass less speaker [6], as propulsion for satellites [7]. But the arc in a circuit can also be an issue: arcing damages relays [8], arc faults damage photovoltaic cells [9] and in airplanes or in homes, arcing faults are responsible of fires [10-12]. As a consequence, researches are focused on arc modeling in circuit [13-26] and arc fault detection algorithms [27-32] for circuit breakers or solid state power controller [29] [30].

Arc models are often developed with plasma physics for very specific applications and they rarely take into account the circuit in which the arc occurs. These models describe the distribution of ions and electrons within the arc, the arc stability and the chemical reactions associated. But, for electronic engineers and researchers, these models are not relevant when studying an arc in a circuit. Then, arc models for circuit are preferred to design arc generator, arc detectors, or arc controllers. To do so, black box models are commonly used. They are based on the well-known Mayr/Cassie arc impedance model [33-35] and many derivatives have been developed [15] [36]. Mayr/Cassie type models provide a qualitative description of the arc in circuits but fail to provide good quantitative results. Mainly because it is difficult to fit Mayr/Cassie models with experimental data [37].

This paper presents a new approach in arc modeling by considering the arc as a circuit element or component. Indeed, we will see that the electric arc behaves similarly to a transistor as well for the polarization process as for the dynamic behavior around the polarization. With this approach, a mathematical model is defined to describe the behavior of the electric arc in power circuits. The model works as well in static or dynamic situations. It is simple because it uses a set of simple equations and allows obtaining very accurate results.

First, we will show how to use the experimental results obtained by Warrington [24] to describe the static arc discharge. Secondly, the dynamic process of the discharge is taken into account to obtain the overall discharge formula. Third, we will discuss the simulation algorithm in order to allow anybody to reproduce the results. In order to evaluate the performance of the model, simulation results and experimental results are discussed in 3 common cases of arc initiation [38]: over voltage ignition, melted bridge ignition and opening contacts ignition. Finally, like for a transistor, we will show how the equivalent small signal model of the arc can be extracted.

II. Background

From a macroscopic point of view, the discharge voltage and current in a circuit evolve as described in figure 1. This figure is called the static discharge characteristic [12] [15] [22] [33]. We can split this characteristic in three distinctive areas (separated by the dot lines in figure 1). One area is comprised between voltages $-V_d$ and V_d. This area corresponds to the resistive part of the static characteristic. The discharge in this case is a glow discharge or it can be a melted bridge. Because both are resistive, we note R_c the resistance for this area. The other two areas are beyond voltages $-V_d$ and V_d and correspond to the arc discharge. In this case the arc resistance is not only a simple resistance but it also depends on the arc current. We note R_{arc} the resistance in those areas. Voltage V_d is call the disruption voltage and I_{Text} is the corresponding current.

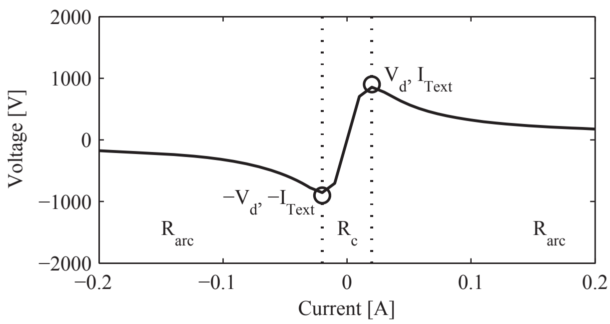

Fig. 1. Representation of a static discharge characteristic.

When initiating a discharge by over voltage, it is first a glow discharge. When the circuit voltage increases, the discharge voltage will cross the disruption voltage V_d. The discharge will so change of area then the discharge becomes an arc discharge. When initiating a discharge by opening a contact or using a melted bridge (such as carbon bridge), in the resistive area, instead of a glow discharge, we simply have the resistance of the melted bridge. We also note R_c the resistance in this case because it leads to the same characteristic of figure 1. So, independently of how the arc is initiated, before the disruption voltage is crossed, the discharge is modeled by a simple resistance R_c. After crossing the disruption voltage, the discharge is modeled by a resistance R_{arc}.

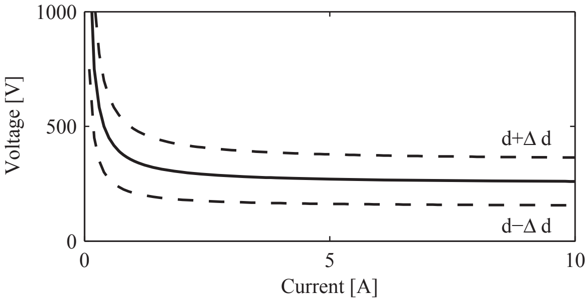

Fig. 2. Static arc characteristic in function of arc length d according to Warrington equation.

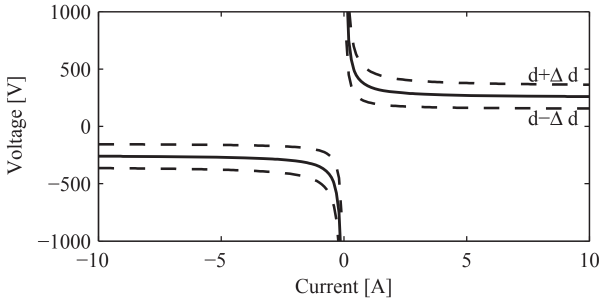

Fig. 3. Static arc characteristic in function of arc length d according to equation 4.

III. Static Arc Analysis

A. Warrington Equations

Warrington has studied the behavior of the static arc [24] [25] and proposed a well-known formula to describe the arc voltage in function of the arc current:

$$V_{arc} = \frac{P_0}{I_{arc}^n} + V_0 \tag{1}$$

Where V_{arc} is the arc voltage, I_{arc} the arc current, V_0 is an electromotive voltage which is a linear function of the arc length d. P_0 is a fit parameter which has the dimension of a power. P_0 is also a linear function of the arc length d.

$$\begin{aligned} P_0 &= A \cdot d + B \\ V_0 &= C \cdot d + D \end{aligned} \tag{2}$$

Parameter n is also a fit parameter which depends on the material of the electrodes (or contacts) used to create the arc. The value of n is usually comprised between 1 and 2. Warrington formula is obtained by experiments. It provides accurate results and we can find numerous experimental data from literature [24] [25] [26]. If we plot this function, we can obtain the curve given in figure 2.

But there are two issues introduced by the Warrington equation; first, if we want to consider a negative current, we must then introduce a condition on the current that changes the sign of V_0:

$$\begin{cases} V_{arc} = P_0/I_{arc}^n + V_0, & I_{arc} > 0 \\ V_{arc} = P_0/I_{arc}^n - V_0, & I_{arc} < 0 \end{cases} \tag{3}$$

This condition on the current is often used in arc modeling [18] [23]. Unfortunately, it may be actually no physical justification to this condition.

Secondly, when looking at equation 1, we see that the voltage going to infinity when the current goes near zero. This is not physically possible. Because first, the arc voltage cannot exceed the maximum voltage imposed by a circuit. And secondly, the voltage cannot be greater than the disruption voltage.

B. Static Arc Equation

To avoid the current condition we rewrite both equations 3 with a unique equation:

$$V_{arc} = \frac{\alpha}{\arctan(\beta I_{arc})} \tag{4}$$

Where parameters α and β play the same role as the Warrington equation parameters P_0 and n. Parameters α is also a linear function of the arc length :

$$\alpha = \gamma \cdot d + \delta \tag{5}$$

Figure 3 shows the result for the proposed equation. One can notice, that if the current is less than one then $\arctan(\beta I_{arc}) \approx \beta I_{arc}$ and by replacing in 4, it is similar to the Warrington formula. The V_0 electromotive voltage of equation 1 is intrinsically taken into account in equation 4 without introducing any consideration on the sign of the current. This is due to the limit of the $\arctan$ function when I_{arc} goes to infinity.

C. Static Discharge Equation

As we have seen, the voltage cannot go to infinity when the current goes to zero. To solve this problem, we simply consider the overall discharge instead of considering only the arc discharge.

If we call R_T the overall discharge resistance, it is then either equal to R_c or equal to R_{arc}. Because the arc resistance R_{arc} is very low in comparison to the resistance R_c (generally from a scale factor of 100 to 1000), we can approximate that both resistances R_{arc} and R_c are present simultaneously during the discharge. The overall discharge resistance R_T is then equivalent to R_c parallel to R_{arc} as described in figure 4.

Assuming that R_c and R_{arc} are in parallel is indeed a good approximation. Because when the current flowing in R_{arc} is low, the resistance R_{arc} is also high. It is as if R_{arc} was not connected in the circuit. At the contrary, when the current flowing in R_{arc} is high, the current flowing in R_c is negligible in comparison to the arc current. Now, it is as if R_c was not connected in the circuit. All is acting as if R_T was either equal to R_c or equal to R_{arc}.

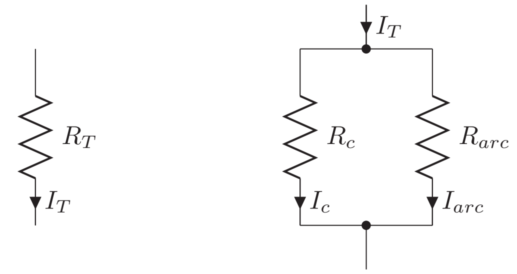

Fig. 4. Equivalent circuit of the overall discharge resistance R_T.

From the equivalent resistance in figure 4, we calculate the total resistance of the discharge R_T:

$$R_T = \frac{R_c R_{arc}}{R_c + R_{arc}} \tag{6}$$

From the equation of the static arc we can find R_{arc}:

$$R_{arc} = \frac{V_{arc}}{I_{arc}} = \frac{\alpha}{\arctan(\beta I_{arc}) I_{arc}} \tag{7}$$

By replacing R_{arc} in 6:

$$R_T = \frac{\alpha R_c}{\arctan(\beta I_{arc}) I_{arc} R_c + \alpha} \tag{8}$$

We also know that:

$$R_T = \frac{V_T}{I_T} \tag{9}$$

So:

$$V_T = \frac{\alpha R_c I_T}{\arctan(\beta I_{arc}) I_{arc} R_c + \alpha} \tag{10}$$

But as we stated before, $R_{arc} << R_c$ then $I_{arc} >> I_c$ and by writing Kirchhoff's law in diagram of figure 4, we have:

$$I_T = I_c + I_{arc} \approx I_{arc} \tag{11}$$

Then replacing I_{arc} by I_T, we can obtain the final equation for the static discharge:

$$V_T = \frac{\alpha R_c I_T}{\arctan(\beta I_T) I_T R_c + \alpha} \tag{12}$$

Figure 5 is the plot of the static discharge described by equation 12. We note F the function that describes the static discharge:

$$V_T = F(I_T) \tag{13}$$

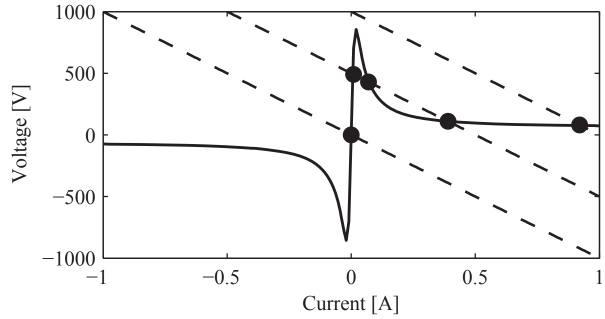

Fig. 5. Overall static discharge characteristic.

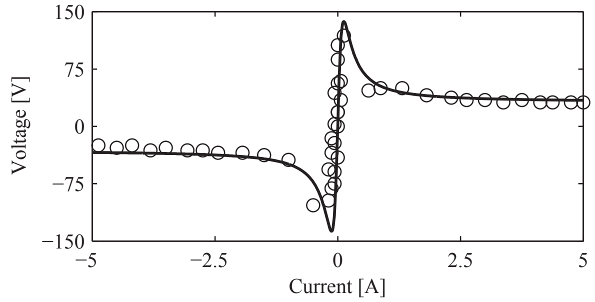

Fig. 6. Static discharge characteristic obtained with basic fitting method versus real data ($\alpha = 49.0874$,$\beta = 1.4614$,$R_c = 2221$).

D. Basic Fitting

The static discharge equation is very easy to manually fit from an experimental VI plot. We have only 3 parameters to determine. To do so, we first measure the limit voltage when the current goes to infinity from an experimental VI plot such as figure 6. We then calculate the first parameter α:

$$\alpha = \pm \frac{\pi}{2} \left(\lim_{I_T \to \pm\infty} V_T \right) \tag{14}$$

Secondly, we calculate R_c from measurement points comprised between V_d and $-V_d$. In over voltage initiation, it can be difficult to measure static points in this area. But only one point is required such as the disruption point V_d,I_{Text} (figure 1). Then we simply calculate $R_c = V_d / I_{Text}$. If we can measure precisely a necessary number of points (it is often the case in contact opening), we may also do a least-square approximation to obtain R_c more precisely.

Finally, knowing α and R_c, we calculate β from the following equation:

$$\beta^2 (\alpha I_{Text}^2) - \beta (R_c I_{Text}^2) + \alpha = 0 \tag{15}$$

We now have the 3 needed parameters α, β and R_c. Figure 6 gives the result for an arc in series initiated by a carbon path in a resistive circuit of 47 Ω with a power supply of 230Vrms. More accurate fitting can be obtained with an appropriate tool such as Matlab Fitting Toolbox with the start parameters (α, β, R_c) calculated previously.

E. Arc Polarization

Polarization of the arc in a circuit is pretty similar to the polarization of a transistor. As an example, we consider a series arc occurring in a simple resistive circuit of resistance R powered by a DC supply voltage V_g. The voltage equation of the circuit is:

$$V_g = RI_T + V_T \tag{16}$$

Expressing this equation in function of V_T gives all the possible discharge voltages allowed by the circuit:

$$V_T = V_g - RI_T \tag{17}$$

The latter is the equation of the load lines of figure 5 where $(-R)$ is the slope. Load lines are drawn for 3 different values of V_g. A load line can cross the static characteristic in one, two, or three points. The cross points, or polarization points, are the solutions for V_T and I_T. In real static cases, when the arc is stable, the solution is generally the one that have the maximum current I_T. In dynamic cases, for example when voltage V_g is varying, the load line is moving on the VI plane and then moves the cross point. Let's say that we now want to solve the circuit equation for a variable voltage V_g with the static arc equation. It means that we consider the circuit as dynamic but not the arc. When the load line is moving, we have to choose one of the possible cross points as solution. To do so, we define a second polarization point V_{arc}, I_{arc} which was the solution at the instant before the present possible solutions V_T, I_T (in the following, notation V_{arc}, I_{arc} corresponds to an overall discharge like it is for V_T, I_T). Then, we calculate for each solution the variation of power:

$$\Delta P = |V_T \cdot I_T - V_{arc} \cdot I_{arc}| \tag{18}$$

Knowing ΔP for all the possible points, we choose the one that implies the minimum of power variation ΔP.

When choosing the right solution, jumps of the polarization point occur. Figures 7 and 8 show two possible jumps. Figure 7 shows the case where the starting point V_{arc}, I_{arc} coincides with the disruption voltage V_d. When the voltage increases, the load line moves up and the final polarization point will be V_T, I_T. The discharge jumps from a glow discharge to an arc discharge. Figure 8 shows the case where the starting polarization point V_{arc}, I_{arc} coincides with the arc extinction point. When the voltage decreases, the load line moves down and the final polarization point will be V_T, I_T. The discharge jumps from an arc discharge to a glow discharge.

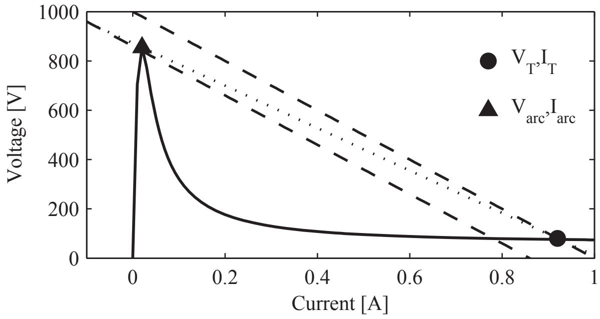

Fig. 7. Transition from glow discharge to arc discharge.

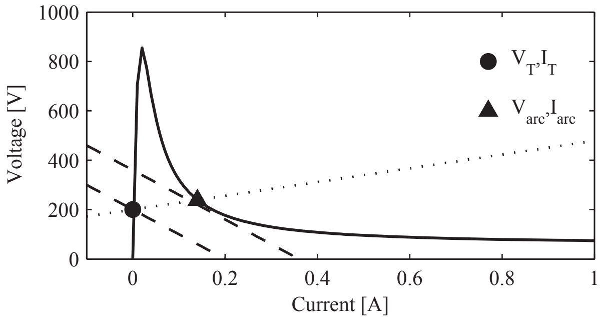

Fig. 8. Transition from arc discharge to glow discharge.

IV. Dynamic Arc Analysis

The main purpose of the dynamic analysis is to explain how the arc resistance evolves in function of time in a circuit. The analysis starts by studying the static equation and calculate how the polarization point is moving when the load is varying or when the power supply is varying and even when the static equation is varying. One common mistake is to consider that point V_{arc}, I_{arc} is just moving on a same trajectory as the static arc equation. A simple experimental VI plot such as the one in figure 17 (d) shows that it is not the case. We can observe from experiments that the real point V_{arc}, I_{arc} can be anywhere on the VI plane. The only fact that we surely know is when circuit parameters or environment parameters stop varying, then the arc stabilizes itself at the static polarization point V_T, I_T. When the polarization point V_T, I_T moves (load is varying or voltage for example), the real arc position V_{arc}, I_{arc} will not follow instantaneously; especially when a jump occurs. The postulate we made is the discharge has temperature inertia which indirectly leads to arc voltage and current inertia. Yet, if we consider V and I like positions in a VI plane, the real V_{arc}, I_{arc} point must have inertia in this VI plane. To obtain the dynamic equation we write the equivalent of the fundamental law of dynamics for the VI point in plane VI:

$$\begin{cases} m\dfrac{d^2V_{arc}(t)}{dt^2} = F_v - k\dfrac{dV_{arc}(t)}{dt} \\ m\dfrac{d^2I_{arc}(t)}{dt^2} = F_i - k\dfrac{dI_{arc}(t)}{dt} \end{cases} \tag{19}$$

Where $d^2V_{arc}(t)/dt^2$, $d^2I_{arc}(t)/dt^2$ is the point acceleration vector, F_v and F_i are components of an hypothetical force F_T that creates the movement of the point. Terms $-kdV_{arc}(t)/dt$, $-kdI_{arc}(t)/dt$ represent the viscosity of the plane in function of the speed and characterized by k. Parameter m is simulating the inertia of the point, it is equivalent to a mass. We can then observe that if the polarization point is not moving, the real point is also not moving when the arc is stable. That means that the force responsible of the creation of the movement of the real point V_{arc}, I_{arc} occurs when the polarization point V_T, I_T moves.

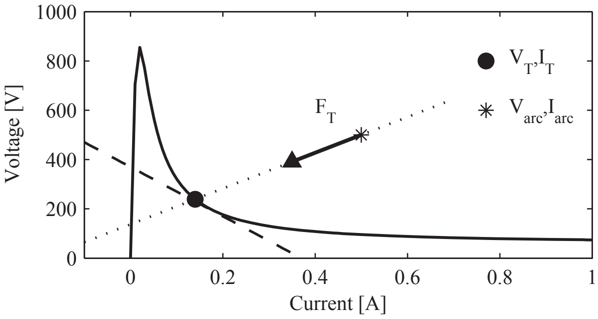

Fig. 9. Trajectory of the V_{arc}, I_{arc} point and position of the static polarization point V_T, I_T.

Figure 9 shows the force F_T created by a move of V_T, I_T and applied on point V_{arc}, I_{arc}.

When decomposing the force F_T in two components F_v and F_i, we see that they are proportional to the variation of the position of the polarization point:

$$\begin{cases} F_v = K\dfrac{dV_T(t)}{dt} \\ F_i = K\dfrac{dI_T(t)}{dt} \end{cases} \tag{20}$$

If we want the forces to be sufficiently strong to move the real point to the polarization point, but also sufficiently weak to not go beyond, then the proportionality ratio K in 20 must be equal to viscosity coefficient k. By replacing K in 20 and replacing F_v and F_i in 19, we obtain:

$$\begin{cases} V_T = V_{arc}(t) + \tau\dfrac{dV_{arc}(t)}{dt} \\ I_T = I_{arc}(t) + \tau\dfrac{dI_{arc}(t)}{dt} \end{cases} \tag{21}$$

Where τ is equal to m/k. Constant τ is representative of a time, it's the arc time constant.

As we discussed, the real point V_{arc}, I_{arc} is not necessary positioned on the static arc characteristic, but by definition the polarization point V_T, I_T must satisfy the characteristic equation:

$$V_T(t) = F\left(I_T(t)\right) \tag{22}$$

So by replacing V_T and I_T in 22 we find the final expression of the dynamic arc equation:

$$V_{arc}(t) = F\left(I_{arc}(t) + \tau\frac{dI_{arc}(t)}{dt}\right) - \tau\frac{dV_{arc}(t)}{dt} \tag{23}$$

V. Simulation Algorithm

The simulation of the arc in a circuit is done by using the equation 23. There are numerous ways to simulate this equation; we choose to present a way which can be done in a Matlab or Octave script file.

The first thing to do is to write the equation of circuit in which the arc is considered. Let's consider a simple RL circuit in which the arc occurs in series. The circuit equation is:

$$V_g(t) = RI_T(t) + L\frac{dI_T(t)}{dt} + V_T \tag{24}$$

The second step is to calculate the associated polarization point V_T,I_T. The polarization point is simply the cross point between the circuit load equation and the static arc characteristic; we have then to solve the system equation:

$$\begin{cases} V_T(t) &= V_g(t) - RI_T(t) - L\dfrac{dI_T(t)}{dt} \\ V_T(t) &= F(I_T(t)) \end{cases} \tag{25}$$

This system equation gives us one, two or three solutions for V_T,I_T.

Third, using the filter-like equations 21 on V_T,I_T, we calculate all the possible V_{arc},I_{arc}. Finally, we choose the right solution V_{arc},I_{arc} using the same method discussed earlier by minimizing the predicted variation of power ΔP.

VI. Simulated and Experimental Results

A. Over Voltage Ignition

The arc is initiated when an over voltage occurs. An over voltage occurs when the voltage is greater than the disruption voltage V_d. When there is no over voltage, the discharge is a glow discharge and the real point V_{arc}, I_{arc} is moving in the resistive area of the static characteristic. When the over voltage occurs, the disruption voltage is crossed and the polarization point jumps as shown in figure 7. Then the discharge is now an arc discharge; the current has a non-negligible value. When the current decreases, the arc extinction point is crossed and the point V_{arc}, I_{arc} jumps to the the resistive area as shown in figure 8. The discharge is trapped again in this area until another over voltage occurs. Figures 10 and 11 show the comparison between the simulated results and the experimental results in the case of an arc initiated with a GDARC [15] in a R circuit with an AC power supply. We can see that simulation results are in accordance with experimental results and that the ignition by over voltage is correctly simulated.

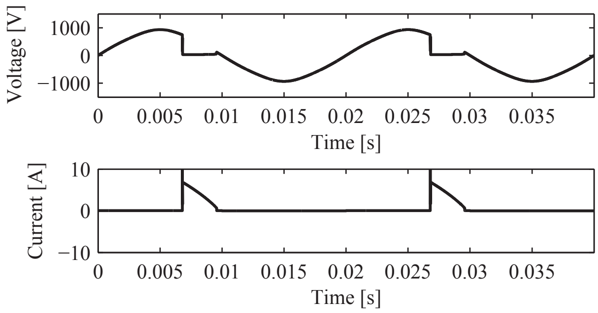

Fig. 10. Voltage and current simulations of series arc initiated by over voltage.

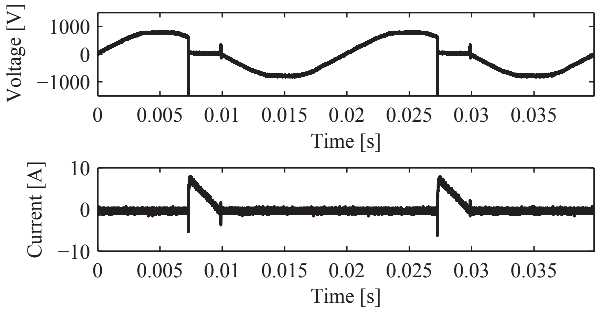

Fig. 11. Experimental voltage and current of series arc initiated by over voltage.

B. Melted Bridge Ignition

A melted bridge is a simple resistance which take place instead of the glow discharge, this resistance is also R_c. The main differences with the over voltage initiation are that R_c is lower than previously and that the disruption voltage V_d is also lower. In most cases the generator voltage is sufficiently high to systematically cross this lower disruption voltage. Figures 12 and 13 show the comparison between the simulated results and the experimental results in the case of a series arc initiated with a carbon path in a R circuit. We can see that simulation results are in accordance with experimental results.

C. Contact Opening Ignition

Contact opening ignition occurs in relays or switches. In a R circuit, before the contacts are open, the current is flowing at a constant value if the generator voltage is constant. In this case, the real point V_{arc}, I_{arc} is placed on the VI plane where $V_{arc} = 0$, and it coincides with V_T, I_T. Indeed, just before the opening the arc voltage is null. When the opening occurs, the polarization point V_T, I_T moves at the cross point of the load line with the minimal static characteristic. The minimal static characteristic is the static characteristic of minimal voltage necessary to have an arc. For example minimum voltage is approximately 12V (it depends on the contacts material). Then the static characteristic varies because it is proportional to arc length d, which also varies when contacts gap increase. Figures 14 and 15 show the results between simulation and experimental signals for a series arc with a DC power supply of 270V and when the length d is varying linearly. If the load R is badly chosen to polarize the arc, the arc will never stops even when the contact is fully open as we can see in figures 14 and 15. Once more, we can see that simulation results are in accordance with experimental results.

D. Arc Time Constant

The arc time constant is representative of the thermal inertia. It represents the delay introduced by the arc as a circuit component. But this is not representative of the delay between the arc current and the arc voltage. Indeed, there's no delay between the arc current and arc voltage. An explanation is given by equation 23: the delay introduced in the current is compensated by the terms $-\tau dV_{arc}/dt$ so that there is no apparent delay between voltage and current. However, also because of the term $-\tau dI_{arc}/dt$, the arc delay can be measured in a R circuit, for example, between the generator voltage and the arc current.

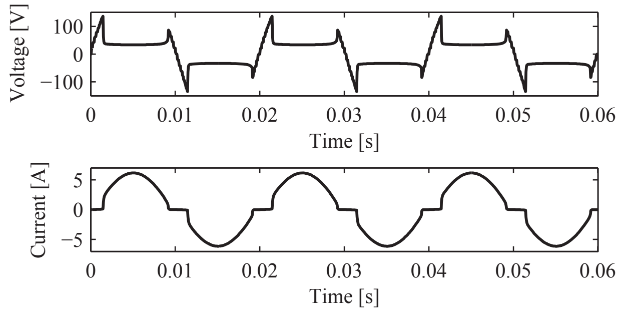

Fig. 12. Voltage and current simulations of series arc in a melted bridge.

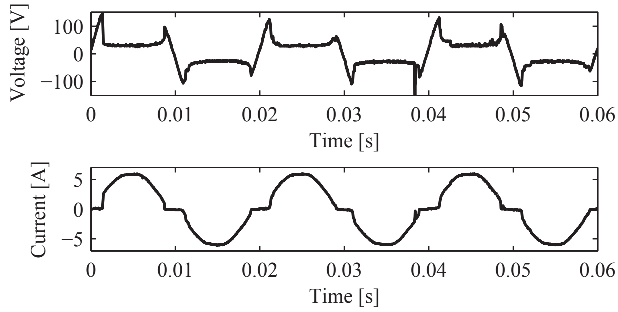

Fig. 13. Experimental voltage and current of series arc in a melted bridge.

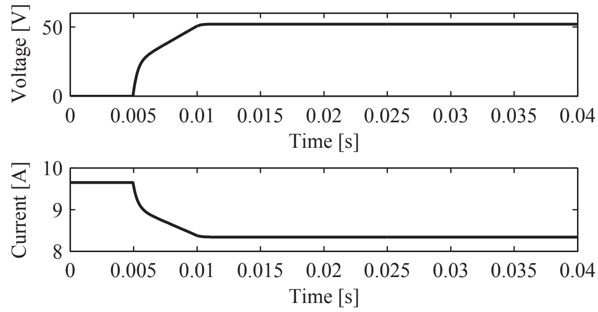

Fig. 14. Voltage and current simulations of series arc when contact opening.

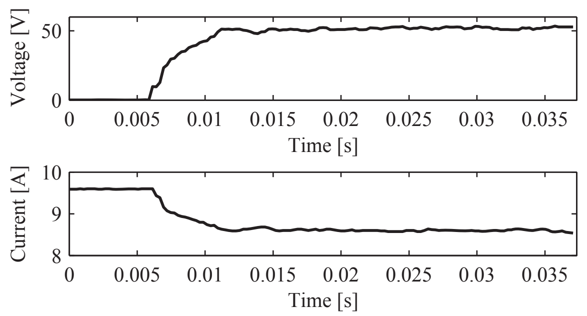

Fig. 15. Experimental voltage and current of series arc when contact opening.

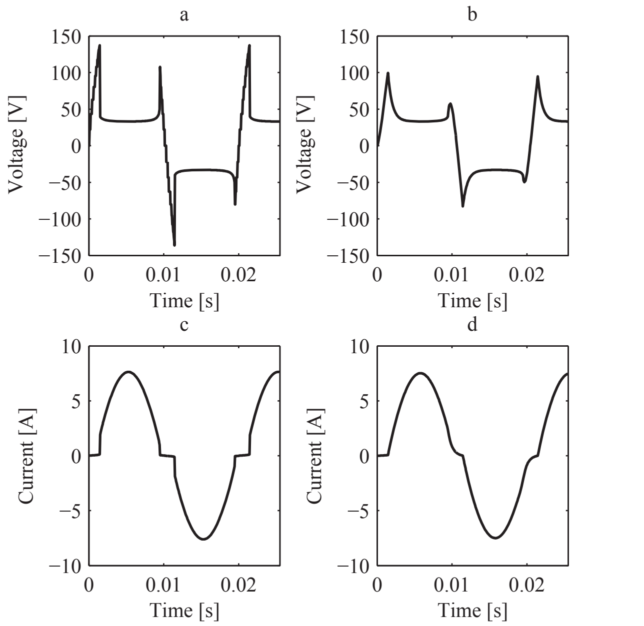

Fig. 16. Currents and voltages of a series arc. Plot a and c correspond to a low arc time constant. Plot b and d correspond to a high arc time constant

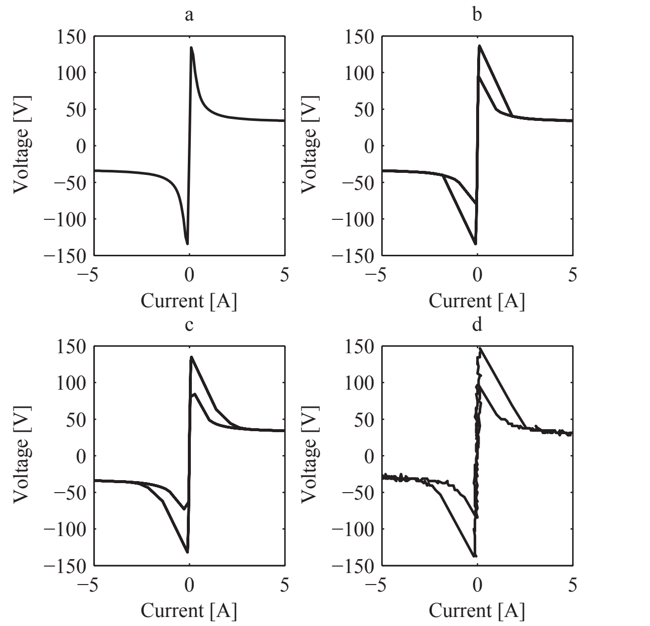

Fig. 17. VI plot of a series arc. Plot a is static characteristic. Plot b is VI plot when arc is considered as static ($\tau \approx 0$). Plot c is VI plot of dynamic arc. Plot d is experimental VI.

We can graphically see the influence of the time constant on arc signals. Figure 16 (a) (c) shows arc signals when arc time constant is low. From equation 23, we see that if $\tau \approx 0$ then the arc is acting approximately like a static arc. Figure 16 (b) (d) shows arc signals when arc time constant is high. The effect on the current waveform is similar to what is observed in a RL Circuit.

Another way to graphically see the influence of the arc time constant is to draw the VI plot. Figure 17 is the VI representation of signals of figure 16. We can observe from Figure 17 that the VI plots of the arc are smoothed as the arc time constant increases.

VII. The Arc as a Component

A. Superposition Principle

In a circuit in which the arc occurs, there are continuous DC sources (voltage or current) that polarized the arc. There are also AC sources that induce arc voltage and current fluctuations. An easy way to analyze the action of the arc in the circuit is to divide the analysis in two parts: one analysis for the DC sources and one for the AC sources. The final results are obtained by adding DC currents and voltages with AC currents and voltages.

B. Small Signal Model

As for the small signal transistor model, we can determine a small signal model for the arc. When the polarization point is defined, the superposition principle allows us to study small variations of arc current around the polarization point. The static characteristic is then considered as linear in this area. We introduce a parameters $g_T = F'(I_T)$. This parameter is the derivative of the function F at polarization current I_T and corresponds to the slope of the linearized characteristic. Equation 23 can be rewritten for small signal as:

$$V_{arc}(t) = g_T I_{arc}(t) + g_T \tau \frac{dI_{arc}(t)}{dt} - \tau \frac{dV_{arc}(t)}{dt} \qquad (26)$$

By observing that g_T and $g_T\tau$ have respectively the dimension of a resistance $R_g(d)$ and an inductance $L_g(d)$, and by defining $V_{em} = -\tau dV_{arc}(t)/dt$ we have:

$$V_{arc}(t) = R_g I_{arc}(t) + L_g \frac{dI_{arc}(t)}{dt} + V_{em} \qquad (27)$$

The latter equation corresponds to the equation of a series RL circuit with an electromotive voltage V_{em}, which diagram is given in figure 18.

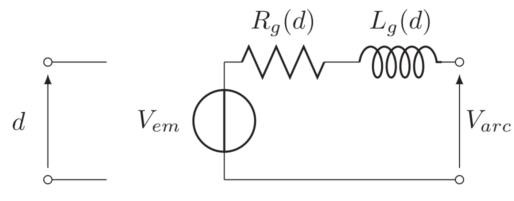

Fig. 18. Small signal circuit of a dynamic arc.

VIII. Conclusion

We have developed a new mathematical representation of an arc in a circuit by introducing the hypothesis of the arc temperature inertia. This temperature inertia introduces voltage and current inertia that allowed us to express the dynamic equation of the arc in a circuit. We have defined the arc time constant and shown how it affects arc signals. We have presented the simulation results of dynamic arcs for 3 different cases of initiation and shown the good agreement with the experimental results. We have provided a basic fitting process and a simulation algorithm that allows anybody to reproduce the results presented in this paper. Finally we have expressed the small signal model of the arc in a circuit. Further work will concern the modeling of the arc time constant τ in the VI plane.

REFERENCES

[1] A. Navarro-Crespin, V.M. Lopez, R. Casanueva, F.J. Azcondo, *Digital Control for an Arc Welding Machine Based on Resonant Converters and Synchronous Rectification.*, IEEE Transactions on Industrial Informatics, Volume:9, Issue: 2, 2012.

[2] J. Wang, C. He, J. Yu, F. Yang, *Development of a Novel Pulsed Arc System for Precision Plasma Cutting*, Proceedings of the IEEE International Conference on Mechatronics and Automation, Aug 2009, Changchun, China.

[3] N. Hariyanto, M. Nurdin, Casanueva, R., G. Alvin Tanthio, *Characteristic Study of Three-phase AC Electric Arc Furnace Model.*, IEEE Conference on Power Engineering and Renewable Energy, 2014.

[4] Y. N. Chang, T. H. Yang, S. Y. Chan, H. L. Cheng, *Design of Electronic Ballast for Short-Arc Xenon Lamps.*, IEEE International Symposium on Industrial Electronics, 2012.

[5] M. Kundrapu, I. Levchenko, K. Ostrikov, M. Keidar, *Simulation of Carbon Arc Discharge for the Synthesis of Nanotubes.*, IEEE Transactions on Plasma Science, Vol. 39, No. 11, Nov. 2011.

[6] Y. Sutton, J. Moore, D. Sharp, N. St. J. Braithwaite, *Looking Into a Plasma Loudspeaker.*, IEEE Transactions on Plasma Science, Vol. 39, No. 11, Nov. 2011.

[7] H. Huang, W. Pan, C. Wu, *Arcjet Thruster Operated With Different Propellants.*, IEEE Transactions on Plasma Science, Vol. 39, No. 11, Nov. 2011.

[8] H. Roman, B. Frank, *Simulation of relay contact bouncing including a short arc model.*, Proceedings of The 27th International Conference on Electrical Contacts, 2014.

[9] J. Flicker, J. Johnson *Electrical Simulations of Series and Parallel PV Arc-Faults.*, IEEE Photovoltaic Specialists Conference (PVSC), 2013.

[10] K. Keller, M. Bailey, K. Wojtek Przytula, B. Jordan, *Aircraft Electrical Power Systems Prognostics and Health Management*, IEEE Aerospace Conference, 2006.

[11] W.S. Moon, J.C. Kim, A. Jo, S.B. Bang, W.S. Koh *Ignition Characteristics of Residential Series Arc Faults in 220-V HIV Wires.*, IEEE Transactions on Industry Applications, Vol. 51, No. 3, May 2015.

[12] R. Landfried, L. Savi, T. Leblanc, P. Teste *Parametric study of electric arcs in aeronautical condition of pressure.*, European Journal on Applied Physics, 2014.

[13] G. Parise, L. Martirano, M. Laurini, *Simplified Arc-Fault Model: The Reduction Factor of the Arc Current.*, IEEE Transactions on Industry Applications, Vol. 49, No. 4, Jul. 2013.

[14] H. Wu, X. Li, D. Stade, H. Schau *Arc Fault Model for Low-Voltage AC Systems.*, IEEE Transactions on Power Delivery, Vol. 20, No. 2, Apr. 2005.

[15] Andrea, J., Schweitzer, P., Martel, J. *Arc Fault Model of Conductance. Application to the UL1699 Tests Modeling.*, 57th Holm Conference on Electrical Contacts, 2011.

[16] T. Gammon, W.J. Lee, Z. Zhang, B.C. Johnson, A. Darwish, N.I. Elkalashy, *A Review of Commonly Used DC Arc Models.*, IEEE Transactions on Industry Applications, Vol. 51, No. 2, Mar. 2015.

[17] H.A. Darwish, N.I. Elkalashy, *Universal Arc Representation Using EMTP*, IEEE Transactions on power delivery, vol 20, n2, april 2005, pp. 81-88.

[18] M. Banejad, R. Allah Hooshmand and M. Torabian Esfahani, *Exponential Hyperbolic Model for Actual Operating conditions of three phase arc furnaces*, American journal of applied sciences, 6, n8, pp. 1539-1547, 2009.

[19] R. Hooshmand, M. Banejad, M. Torabian Esfahani, *A new time model domain model for electric arc furnace*, journal of electrical engineering, vol 59, n4, pp. 195-202, 2008.

[20] S. Hutter, I. Uglesic , *Universal arc resistance model, Zagreb for EMTP*, 19th International Conference on Electricity Distribution, Vienna, 21-24 may 2007.

[21] S. Berger, *Mathematical approach to model rapidly elongated free-burning arcs in air in electric power circuits.*, ICEC 2006, , Sendai, 6-9 June 2006.

[22] G.I. Ospina, D. Cubillos, L. Ibanez, *Analysis of arcing fault models, Transmission and Distribution Conference and Exposition.*, Bogota, 10 oct 2008.

[23] N. Zamanan, J.K. Sykulski, *Modelling arcing high impedances faults in relation to the physical processes in electric arc*, 6th WSEAS international conference on power system, Lisbon, 2006.

[24] V. Terzija, V. Koglin, *On the modeling of long arc in still air and arc resistance calculation.*, IEEE Transactions on Power Delivery, 1012-1017, 2004.

[25] V. Terzija, V. Koglin, *A new approach to arc resistance calculation.*, Journal of Electrical Engineering, Volume 83, Issue 4 , 187-192, 2001

[26] V.D. Andrade, L. Sorrentino, *Typical expected values of the fault resistance in power systems.*, Transmission and Distribution Conference and Exposition: Latin America (TD-LA),IEEE/PES (pp. 602-609),2010

[27] J. Lezama, P. Schweitzer, S. Weber, E. Tisserand, P. Joyeux, *Arc Fault Detection Based on Temporal Analysis.*, IEEE Conference on Electrical Contacts, 2014.

[28] G.S. Seo, K.A. Kim, K.C. Lee, K.J. Lee, B.H. Cho, *A New DC Arc Fault Detection Method Using DC System Component Modeling and Analysis in Low Frequency Range.*, IEEE Applied Power Electronics Conference and Exposition (APEC), 2015.

[29] M. Xie, X. Zhang, Y. Dong, W. Li, *Arc Fault Detection for DC Solid State Power Controllers.*, IEEE Conference and Exposition on Transportation Electrification Asia-Pacific (ITEC Asia-Pacific), 2014.

[30] J. Andrea, O. Zirn, M. Bournat, *Arc Fault Detection for DC Solid State Power Controllers.*, IEEE 58th Holm Conference onElectrical Contacts, 2012.

[31] M. Michalik, W. Rebizant, M. Lukowicz, *Wavelet transform approach to high impedance fault detection in MV Networks.*, Power Tech, 2005 IEEE Russia, June 2005

[32] T.M. Lai, L.A. Snider, E. Lo *Wavelet transform based relay algorithm for the detection of stochastic high impedance faults Electric power system research.*, vol 76, pp 6626-633, 2006.

[33] H. Ayrton, *The Electric Arc.*, Printing and Publishing Company, London, 1902.

[34] A.M. Cassie, *Theorie nouvelle des arcs de rupture et de la rigidite des circuits.*, CIGRE Report, 102, 1939.

[35] O. Mayr, *Beitrage zur theorie des statischen und des dynamischen Lichtbogens.*, Archiv fr Elektrotechnik, vol Band 37, Heft 12, pp 588-608, 1943.

[36] P.H. Schavemaker, L. Van der Sluis, *An improved mayr type arc model based on current zero measurement*, IEEE Transactions on Power delivery, vol 15, n2, apr 2000.

[37] S. Maximov, V. Venegas, J.L. Guardado, *A Method for Obtaining the Electric Arc Model Parameters for SF6 Power Circuit Breakers*, IEEE EUROCON, 2009.

[38] Underwriters Laboratories Inc. (UL), *UL Standard for Safety for Arc-Fault Circuit-Interrupters*, ANSI UL 1699, Second Edition, 2008.